

21cm Cosmology

Mario G. Santos^{1,2,5}, David Alonso³, Philip Bull⁴, Stefano Camera^{5,1},
and Pedro G. Ferreira³

¹Department of Physics, University of Western Cape, Cape Town 7535, South Africa

²SKA SA, 3rd Floor, The Park, Park Road, Pinelands, 7405, South Africa
email: mgrsantos@uwc.ac.za

³Astrophysics, University of Oxford, DWB, Keble Road, Oxford OX1 3RH, UK

⁴Institute of Theoretical Astrophysics, University of Oslo,
P.O. Box 1029 Blindern, N-0315 Oslo, Norway

⁵CENTRA, Instituto Superior Técnico, Universidade de Lisboa, Portugal

Abstract. A new generation of radio telescopes with unprecedented capabilities for astronomy and fundamental physics will be in operation over the next few years. With high sensitivities and large fields of view, they are ideal for cosmological applications. We discuss their uses for cosmology focusing on the observational technique of HI intensity mapping, in particular at low redshifts ($z < 4$). This novel observational window promises to bring new insights for cosmology, in particular on ultra-large scales and at a redshift range that can go beyond the dark energy domination epoch. In terms of standard constraints on the dark energy equation of state, telescopes such as Phase I of the SKA should be able to obtain constraints about as well as a future galaxy redshift surveys. Statistical techniques to deal with foregrounds and calibration issues, as well as possible systematics are also discussed.

Keywords. instrumentation: interferometers, methods: data analysis, cosmology: observations, (cosmology:) diffuse radiation, (cosmology:) large-scale structure of universe, radio lines: galaxies.

1. Introduction

In recent years we have seen a dramatic improvement in the constraints imposed on the cosmological parameters, entering a phase sometimes called of precision cosmology. One of the most prominent examples of this are the CMB results from WMAP (Hinshaw *et al.* 2013) and more recently the Planck satellite (Planck Collaboration *et al.* 2013b) providing sub-percent constraints on several parameters. The current picture shows an Universe well described by only 6 parameters and a dominant dark energy component very similar to a cosmological constant.

A great effort is now underway to push the boundaries of this standard model and obtain information that can give us new insights into the true nature of these cosmological parameters. Examples are the properties of dark energy, the possibility of modifications to General Relativity or the nature of the primordial fluctuations of the Universe. One of the most accessible methods to probe the energy content and large-scale structure evolution of the Universe is through large galaxy surveys which can be used as tracers of the underlying dark matter distribution. Several surveys are now being done or in preparation, in particular: BOSS (SDSS), DES, and the Euclid satellite†. These surveys are based on imaging of a large number of galaxies at optical or near-infrared wavelengths combined with redshift information to provide a 3-dimensional position of the galaxies.

† www.sdss3.org/surveys/boss.php; www.darkenergysurvey.org; www.euclid-ec.org

Although large radio-galaxy surveys do exist (FIRST, NVSS)[‡], they lack direct redshift information from the radio which can seriously impair their usefulness for cosmological applications. The solution will be to use the hydrogen (HI) 21cm line to provide the redshift information from radio surveys (this HI emission comes from the hydrogen spin-flip hyperfine transition at a rest wavelength of 21 cm). HI pervades space from the time of recombination up to the present day. At late times the Universe has reionised, and so the bulk of the neutral hydrogen is thought to reside in comparatively dense gas clouds (damped Lyman-alpha systems) embedded in galaxies, where it is shielded from ionising UV photons. HI is therefore essentially a tracer of the galaxy distribution. At a rest frequency of 1420 MHz, telescopes probing the sky between this and 250 MHz would be able to detect galaxies up to redshift 5 at wavelengths that are mostly immune to obscuration by intervening matter. The problem is that this emission line is usually quite weak: at $z = 1.5$ most galaxies with a HI mass of $10^9 M_{\odot}$ will be observed with a flux density of $\sim 1\mu\text{Jy}$ (see Obreschkow *et al.* 2009). In order to obtain game changing cosmological constraints, experiments with sensitivities better than $\sim 10\mu\text{Jy}$ will then be required so to provide enough galaxies to beat shot noise at the cosmic variance level (Abdalla *et al.* 2010). Although near term radio telescopes such as ASKAP and MeerKAT should be able to achieve such sensitivities on deep single pointings, it will require a much more powerful telescope such as SKA Phase 2[¶], to integrate down to the required sensitivity over the visible sky in a reasonable amount of time. This would imply that one would need to wait until then to use radio telescopes for Cosmology.

Experiments used for galaxy surveys are threshold surveys in that they set a minimum flux above which galaxies can be individually detected. Instead we could consider measuring the integrated 21cm emission of several galaxies in one angular pixel on the sky and for a given frequency resolution. For a reasonably large 3d pixel (angular times frequency) we expect to have several HI galaxies in each pixel so that their combined emission will provide a larger signal. For instance, if we are interested on scales relevant for baryon acoustic oscillations (~ 150 Mpc), resolutions of around 30 arc min in angle and 1 MHz in frequency are enough. Moreover we can use statistical techniques, similar to what has been applied for instance to CMB experiments, to measure quantities in the low signal to noise regime. By not requiring the detection of each galaxy, the specification requirements imposed on the telescope will be much less demanding. This is what has been commonly called as an intensity mapping experiment. The result is a map of large-scale fluctuations in 21cm intensity, similar to a CMB map, except now the signal is also a function of redshift. Combined with the high frequency (and thus redshift) resolution of modern radio telescopes, this *intensity mapping* (IM) methodology makes it possible to efficiently survey extremely large volumes (Battye *et al.* 2004; McQuinn *et al.* 2006; Chang *et al.* 2008; Mao *et al.* 2008; Loeb & Wyithe 2008; Pritchard & Loeb 2008; Wyithe & Loeb 2008; Wyithe *et al.* 2008; Peterson *et al.* 2009; Bagla *et al.* 2010; Seo *et al.* 2010; Lidz *et al.* 2011; Ansari *et al.* 2012; Battye *et al.* 2013). By not requiring galaxy detections, the intensity mapping technique transfers the problem to one of foreground removal: how to develop cleaning methods to remove everything that is not the HI 21cm signal at a given frequency. This in turn also impacts on the calibration requirements of the instrument. In this paper, we discuss the cosmological applications available with HI IM as well as the statistical challenges that one will have to overcome in order to measure this signal at the required precision level.

[‡] sundog.stsci.edu; www.cv.nrao.edu/nvss

[¶] www.atnf.csiro.au/projects/askap; www.ska.ac.za/meerkat; www.skatelescope.org

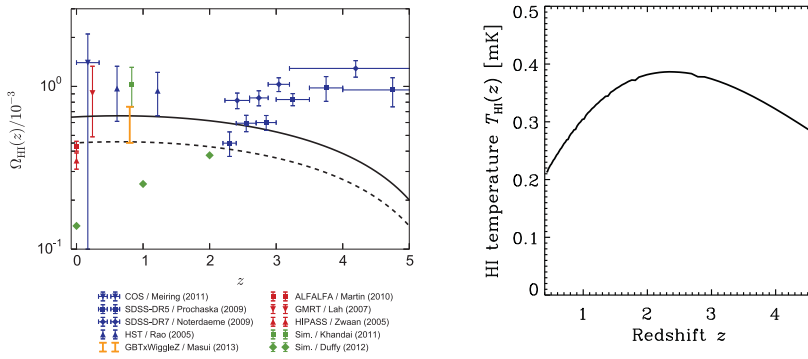


Figure 1. The evolution with redshift of the HI density parameter (left) and the HI temperature signal (right).

2. The HI intensity mapping signal

Radio telescopes measure flux density – the integral of the source intensity, I_ν , over the solid angle of the telescope beam. In the Rayleigh-Jeans limit, this can be converted into an effective brightness temperature, $T_b = c^2 I_\nu / 2k_B \nu^2$, that can be split into a homogeneous part and a fluctuating part, $T_b = \bar{T}_b (1 + \delta_{HI})$, where

$$\bar{T}_b = \frac{3}{32\pi} \frac{hc^3 A_{10}}{k_B m_p \nu_{21}^2} \frac{(1+z)^2}{H(z)} \Omega_{HI}(z) \rho_{c,0}. \tag{2.1}$$

$\Omega_{HI}(z)$ is the comoving neutral hydrogen density in units of the critical density today (see 1) and δ_{HI} are the fluctuations in the neutral hydrogen mass. At late times, most of the neutral hydrogen content of the Universe is expected to be localised to dense gas clouds within galaxies, where it is shielded from ionising photons. We therefore expect HI to be a biased tracer of the dark matter distribution, just as galaxies are. This allows us to write the HI density contrast as $\delta_{HI} = b_{HI} \star \delta_M$ (where δ_M is the total matter density perturbation, and \star denotes convolution, accounting for the possibility of scale- and time-dependent biasing). Figure 1 shows the expected evolution of the average signal as a function of redshift.

Because the HI intensity is measured as a function of frequency (and thus redshift) rather than comoving distance, we must also account for redshift space distortions (RSDs) caused by the peculiar velocities of the clouds and the galaxies in which they reside. Following Kaiser (1987), we write the (Fourier-transformed) redshift-space HI contrast as

$$\delta_{HI}(\mathbf{k}) = (b_{HI} + f\mu^2) \exp(-k^2 \mu^2 \sigma_{NL}^2 / 2) \delta_M(\mathbf{k}), \tag{2.2}$$

where $\mu \equiv k_{||} / k$ and the flat-sky approximation has been used again. We have assumed that the HI velocities are unbiased. The linear growth factor, f , is a key observable, telling us much about the growth of structure on linear scales. The exponential term accounts for the ‘‘Fingers of God’’ effect due to uncorrelated velocities on small scales, which washes out structure in the radial direction past a cutoff scale parametrised by the non-linear dispersion, σ_{NL} .

One key uncertainty is the behaviour of the HI bias, b_{HI} . The bias depends on the size of host dark matter haloes; if a halo is too small, gas clouds would be unable to gain sufficient density to shield themselves and keep the hydrogen neutral. The halo dependence can be modelled using the halo mass function with an appropriate lower mass cutoff (or lower rotation velocity); see (Bagla *et al.* 2010) for example. There are

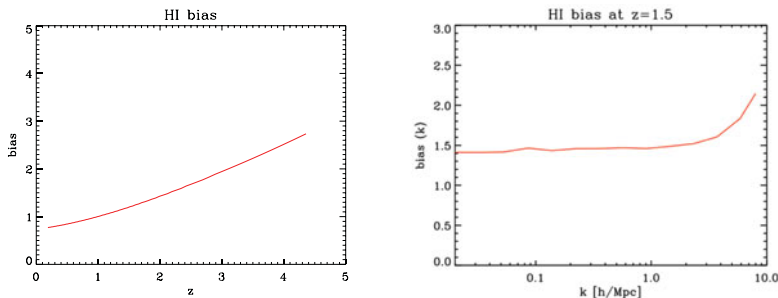


Figure 2. The evolution of the bias as a function of redshift (left) and scale (right).

a few candidate models for the evolution of the bias as a function of redshift that fit the current constraints from observations (Switzer *et al.* 2013) or are calibrated against simulations (Wilman *et al.* 2008), but there is considerable disagreement between them. Unless stated otherwise, we will use a linear bias model for the rest of the paper, and – rather conservatively – marginalise over the value of b_{HI} separately in each redshift bin.

Another major uncertainty is in the HI density fraction, $\Omega_{\text{HI}} = \rho_{\text{HI}}/\rho_{c,0}$. The current best constraints on the HI fraction come from Switzer *et al.* (2013), who find

$$\Omega_{\text{HI}} b_{\text{HI}} = 4.3 \pm 1.1 \times 10^{-4}$$

at the 68% confidence level at $z = 0.8$. This constitutes a relatively large uncertainty in the overall amplitude of the HI signal and, correspondingly, the signal-to-noise that can be achieved by a given experiment. For the rest of the paper we will adopt a fiducial value of $\Omega_{\text{HI},0} = 6.5 \times 10^{-4}$. Figure 1 shows the expected HI bias and Ω_{HI} for a few models as well as current measurements. Given the low resolution of these experiments, it should be a good enough approximation to consider that the total HI mass is a function of the host dark matter halo mass (a redshift dependence can also be included).

Once $M_{\text{HI}}(M, z)$ has been specified, we can calculate Ω_{HI} , the HI bias, and HI brightness temperature in a consistent manner. For the mass function, the most straightforward ansatz is to assume that it is proportional to the halo mass – the constant of proportionality can then be fitted to the available data. Even in this case, however, we need to take into account the fact that not all halos contain galaxies with HI mass. Following (Bagla *et al.* 2010), we assume that only halos with circular velocities between 30 – 200 kms^{-1} are able to host HI.

3. Experiments

First attempts at using intensity mapping have been promising, but have highlighted the challenge of calibration and foreground subtraction. The Effelsberg-Bonn survey (Kerp *et al.* 2011) has produced a data cube covering redshifts out to $z = 0.07$, while the Green Bank Telescope (GBT) has produced the first (tentative) detection of the cosmological signal through IM by cross-correlating with the WiggleZ redshift survey (Chang *et al.* 2010; Switzer *et al.* 2013; Masui *et al.* 2013). As probes to constrain cosmological parameters these measurements are, as yet, ineffective, but they do point the way to a promising future.

We can divide the intensity mapping experiments into two types: dish surveys and interferometers. In single dish surveys (auto-correlations) each pointing of the telescope gives us one single pixel on the sky (though more dishes or feeds can be used to increase the field of view). It has the advantage that can give us large scale modes by scanning

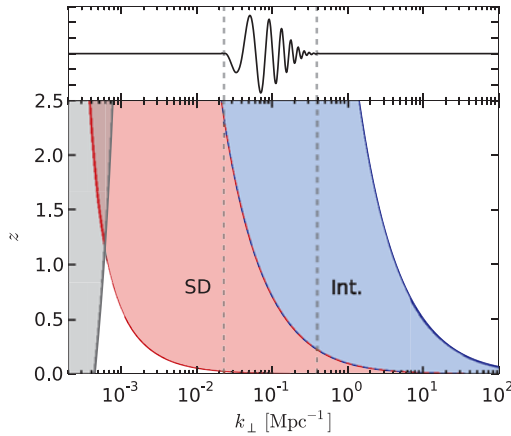


Figure 3. Redshift evolution of the minimum/maximum transverse scales (filled regions) for illustrative interferometer (blue) and single-dish (red) experiments. The BAO are plotted for comparison. The dishes have diameter $D_{\text{dish}} = 15\text{m}$, the min./max. interferometer baselines are $D_{\text{min}} = 15\text{m}$ and $D_{\text{max}} = 1000\text{m}$, and the survey has bandwidth $\Delta\nu = 600\text{ MHz}$ and area $S_{\text{area}} = 25,000\text{ sq. deg.}$ The shaded grey region denotes superhorizon scales, $k < k_H = 2\pi/r_H$.

the sky. Since brightness temperature is independent of dish size we can achieve the same sensitivity with a smaller dish although that will in turn limit the angular resolution of the experiment (a 30 arc min resolution at $z \sim 1$ would require a dish of about 50 m in diameter). One example is the GBT telescope as described above. BINGO (Battye *et al.* 2013) is a proposed 40m multi-receiver single-dish telescope to be set in South America and aimed at detecting the HI signal at $z \sim 0.3$.

Interferometers basically measure the Fourier transform modes of the sky. They have the advantage of easily providing high angular resolution as well being less sensitive to systematics that can plague the auto-correlation power. On the other hand, the minimum angular scale they can probe is set by their shortest baseline which can be a problem when probing the BAO scales. One example of a purpose built interferometer for intensity mapping is CHIME a proposed array, aimed at detected BAO at $z \sim 1$, made up of $20 \times 100\text{m}$ cylinders, based in British Columbia, Canada. The pathfinder has 2 half-length cylinders, and the full experiment has 5 (CHIME Collaboration 2012).

The next generation of large dish arrays can also potentially be exploited for HI intensity mapping measurements. Such is the case of MeerKAT and ASKAP. However, these interferometers do not provide enough baselines on the scales of interest (5m to 80m) so that their sensitivity to BAO will be small. The option is to use instead the auto-correlation information from each dish, e.g. make a survey using the array in single dish mode. Figure 3 shows the scales that can be probed by an array with 15m dishes in single dish and interferometer mode. The large number of dishes available with these telescopes will guarantee a large survey speed for probing the HI signal.

The ultimate example of this approach will be SKA1, the first phase of the SKA telescope, to be built in 2018. This will comprise of 254 single pixel feed dishes to be built in South Africa (SKA1-Mid) and 96 dishes fitted with 36 beam PAFs to increase the field of view to be set in Australia (SKA1-Sur). A HI intensity mapping survey will turn SKA phase 1 into a state of the art cosmological probe. It will allow SKA1 to make detailed measurements of Baryon Acoustic Oscillations and redshift space distortions at several redshifts as well as detect dark matter fluctuations on ultra-large scales past the equality peak and on super-horizon scales. This will make SKA1 capable of addressing

crucial questions in Cosmology such as the nature of dark energy and modified gravity, at a level competitive with concurrent experiments as well as push limits on non-standard parameters such as the curvature of the Universe, primordial non-Gaussianity or General Relativistic corrections on ultra-large scales.

4. Forecasts for late time cosmology

Once the BAO are detectable, it will become possible to use IM experiments for precision cosmological measurements. By using the BAO as a ‘standard ruler’ in the radial and transverse directions, one can constrain the expansion rate, $H(z)$, and angular diameter distance, $D_A(z)$, respectively. These functions of redshift encode crucial information about the energy content and geometry of the Universe; in particular, measurements at $z \lesssim 1.5$ provide a wealth of information about the possible evolution of dark energy, parametrised by its equation of state, $w(z)$. One of the central tasks of observational cosmology over the coming decade will be to determine $w(z)$ to high precision. The spatial curvature of the Universe, Ω_K , can also be pinned down by distance measurements over an even wider redshift range, providing a useful consistency check on the inflationary paradigm.

RSDs, in addition to having a role in separating the radial and transverse BAO, also provide valuable cosmological information in their own right. They are sensitive to the growth rate of structure, $f(z)$, which is a key observable for testing deviations from General Relativity on cosmological scales. Thanks to the high frequency (and thus redshift) resolution of modern radio receivers, experiments like the SKA can be expected to measure RSDs to high precision as well.

Both BAOs and RSDs are now routinely measured in large optical galaxy redshift surveys (e.g. Blake *et al.* (2012); Dawson *et al.* (2013)), which are continually increasing in size and precision. By measuring the same quantities over a wider sweep of redshifts, for a larger fraction of the sky, a HI intensity mapping survey on SKA1 has the potential to provide both competitive constraints on key cosmological parameters like $w(z)$, and vital cross-checks for future optical surveys. Indeed, as surveys begin to come up against the limits imposed by cosmic variance and difficult-to-model systematic effects, it will become particularly important to leverage “multi-tracer” approaches (McDonald & Seljak 2009).

While contingent on the relative importance of foreground contamination and calibration uncertainties, as discussed in subsequent sections, one can nevertheless get some handle on the expected performance of future IM surveys using the Fisher forecasting technique. The basic idea of Fisher forecasting is to derive a Gaussian approximation of the joint likelihood for a set of parameters, given a fiducial model of the expected signal and the noise properties of an experiment. The power of this approach lies in its simplicity; important aspects of measurements such as parameter degeneracies can be taken into account without the need for computationally-expensive simulations (although ultimately these are needed to understand the expected performance characteristics of an experiment in detail).

A Fisher forecasting formalism for intensity mapping was developed in Bull *et al.* (2014), based on a similar method for characterising galaxy redshift surveys. In Fig. 4, we use this method to forecast the expected constraints on the dark energy equation of state parameters and the growth rate for two example SKA1 configurations in single-dish mode. A 10,000 hour IM survey on SKA1 will offer comparable precision to a large multi-year Stage IV galaxy survey such as Euclid or WFIRST in around the same timeframe. Assuming that various statistical challenges can be overcome, intensity mapping therefore

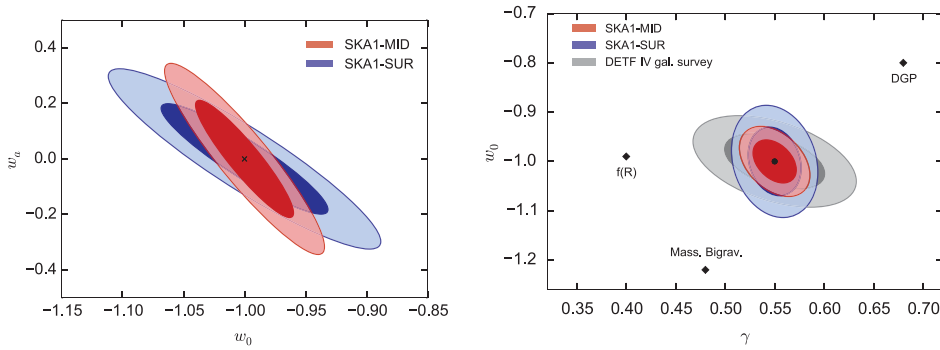


Figure 4. Left: Fisher forecasts for a parametrisation of the dark energy equation of state, $w(z) \approx w_0 + w_a(1 - a)$, for two example SKA1 intensity mapping surveys. Right: Forecasts for w_0 and the growth index, γ , (where $f \approx \Omega_M^\gamma(z)$) for the same surveys, with example modified gravity models and a forecast for a DETF Stage IV galaxy redshift survey shown for comparison. Each IM survey is for 10,000 hours over 25,000 sq. deg. of the sky. The redshift ranges depend on the frequency coverage of the instrument; for band 2 of both SKA1-MID and SUR these are $0 \leq z \leq 0.5$ and $0.2 \leq z \leq 1.2$ respectively.

has the potential to become a leading precision cosmological probe over the coming decade.

5. Cosmology on ultra-large scales

Besides being a valuable tool for standard cosmological analyses, intensity mapping is incomparable in probing the Universe's largest scales. Constraints on the properties of density perturbations on extremely large cosmic scales can greatly improve our understanding of the very early Universe. Indeed, these scales are well within the linear régime, thus being uncontaminated by non-linear growth of structure. Furthermore, the poorly understood effects of baryons can be safely neglected.

Ultra-large scales are utterly difficult to access with conventional experiments. On the one hand, the potentiality of CMB experiments is wasted by cosmic variance. On the other hand, for large volumes of the Universe we not only need wide fields of view, but also deep observations—in order to probe small perpendicular wavenumbers as well as transverse ones—and this is a problem for usual galaxy redshift surveys. Indeed, it is hard to achieve the required sensitivity at large redshifts over wide areas of the sky. On the contrary, if we forego the identification of individual galaxies, we can greatly speed up the observation and detection of the large-scale structure. Intensity mapping experiments are thus sensitive to density fluctuations at a redshift range observationally difficult to span for standard galaxy surveys (Seo *et al.* 2010).

Amongst the most interesting phenomena occurring on the largest cosmic scales we can list the general relativistic corrections to cosmological observables, modified gravity signatures and large-scale biasing effect entailed to primordial non-Gaussianity. General relativistic effects can significantly deviate from the standard, Newtonian prediction on ultra-large cosmic scales. A measurement of such effects will be a powerful, additional proof of the goodness of Einstein's general relativity. Conversely, it has been argued that modifications of the behaviour of gravity on cosmological distances—which can possibly explain the late-time accelerated expansion of the cosmos with need of neither a cosmological constant nor DE—may hide close to the horizon scale. Thus, it is imperative to scan properly all the cosmological scales in the search for deviation from general

relativity. Finally, it is also renowned that most models of inflation predict slightly non-Gaussian initial conditions, whose effects on the clustering of galaxies and galaxy clusters are the strongest on ultra-large scales.

Regarding the potentiality of intensity mapping experiments for detecting primordial non-Gaussianity, Camera *et al.* (2013) scrutinised several configurations for both single dish surveys and interferometers. They demonstrated that oncoming experiments such as those leading to the Square Kilometre Array will be capable of reaching such a level of accuracy on the measurement of the primordial non-Gaussianity parameter, f_{NL} to be able to discriminate operatively amongst competing inflationary scenarios. This is particularly true when resorting to large surveys of the sky using single dish mode until $z \sim 3$.

6. Statistical challenges I: Foregrounds

One of the most important challenges facing HI intensity mapping is the presence of foregrounds (both galactic and extra-galactic) with amplitudes several orders of magnitude larger than the signal to be measured. The statistical properties, as well as the frequency dependence of these foregrounds differs significantly from those of the signal, and therefore there is hope that they can be successfully subtracted (Di Matteo *et al.* 2002; Oh & Mack 2003; Santos *et al.* 2005; Morales *et al.* 2006; Wang *et al.* 2006; Gleser *et al.* 2008; Jelić *et al.* 2008; Liu *et al.* 2009; Bernardi *et al.* 2009, 2010; Jelić *et al.* 2010; Moore *et al.* 2013; Wolz *et al.* 2014; Shaw *et al.* 2013). Nevertheless, this foreground subtraction is a potential source of systematic effects that could limit the observational power of intensity mapping for cosmology. Evaluating and modelling these systematics is therefore an essential step in the observational pipeline that requires the use of simulated realisations of these foregrounds.

It has become the norm in the analysis of Cosmic Microwave Background (CMB) data to construct efficient simulations which can then be used to understand the analysis pipeline for any given experiment (Hinshaw *et al.* 2013; Planck Collaboration *et al.* 2013a). By including different foreground contaminants and instrumental systematic effects in the simulation, it is then possible, via Monte Carlo techniques, to accurately estimate the various biases that may enter the final result. In this spirit, Alonso *et al.* (2014) presented a computer code to generate fast mock realizations of the intensity mapping signal, as well as its most relevant foregrounds. The method is similar to those used in galaxy redshift surveys to produce mock catalogs, and is based on generating a lognormal realization of the density field of neutral hydrogen. Through this method it is possible to implement the most important effects (e.g.: the bias of HI with respect to the matter density, the lightcone evolution of the density field, redshift space distortions, frequency decorrelation in the foregrounds, etc.) at a very low computational cost. Five different types of foregrounds have been implemented in the present version of the code: unpolarized and polarized galactic synchrotron, galactic and extragalactic free-free emission and emission from extragalactic point radio sources. Their modelling was based partly on the parametrization of Santos *et al.* (2005) and on the methods used by other groups to simulate radio foregrounds (Jelić *et al.* 2010; Shaw *et al.* 2013, 2014).

The problem of foregrounds has been addressed in the literature mainly for the EoR case, but few studies exist regarding the range of frequencies relevant for intensity mapping. The different algorithms that have been proposed to date can be classified into *blind* (Wang *et al.* 2006; Switzer *et al.* 2013; Chapman *et al.* 2012) and *non-blind* (Liu & Tegmark 2011; Shaw *et al.* 2013) methods, depending on the kind of assumptions made about the nature of the foregrounds (e.g. whether only general properties such as

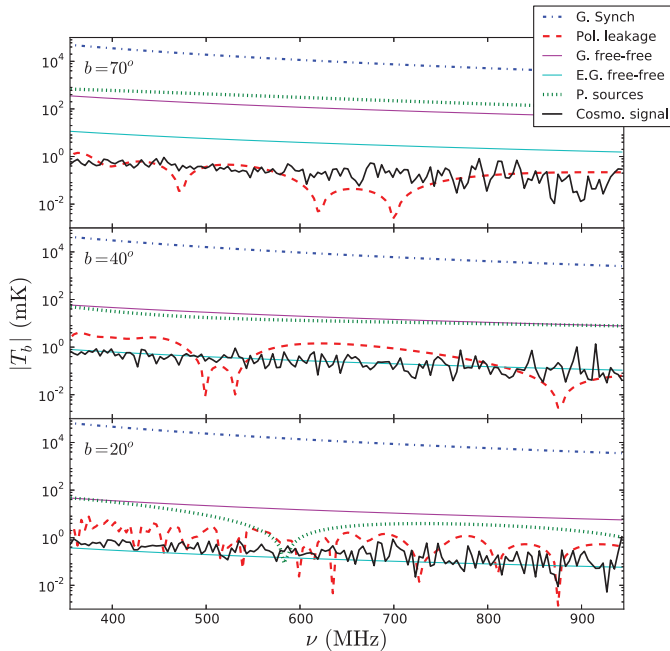


Figure 5. Frequency-dependence of the different foregrounds and the cosmological signal along lines of sight with different galactic latitudes (given in the top right corner of each panel), according to the simulations of Alonso *et al.* (2014). The effect of Faraday decorrelation on the polarized synchrotron emission increases as we approach the galactic plane, making the subtraction of the polarization leakage more challenging.

smoothness and degree of correlation are assumed or whether a more intimate knowledge of the foreground statistics is needed). Recently Wolz *et al.* (2014) studied the effectiveness of the FastICA method for intensity mapping, finding that foreground removal is indeed possible, although it may induce a residual bias on large angular scales that could prevent a full analysis based on the shape of the temperature power spectrum. This result is not surprising: most relevant foregrounds are (fortunately) exceptionally smooth and therefore it should be possible to distinguish them from the much “noisier” cosmological signal. Any foreground residual will probably be dominated by galactic synchrotron emission, which is most relevant on large angular scales.

Of greater concern is the problem of polarization leakage. Linearly polarized radiation changes its polarization angle in as it traverses the galaxy due to Faraday rotation, an effect that is frequency-dependent and therefore not spectrally smooth. Hence, if part of the polarized synchrotron intensity is leaked into the unpolarized signal due to instrumental issues, it could become an extremely problematic “foreground” (see figure 5). This, together with other frequency-dependent instrumental effects (e.g. a ν -varying beam) could turn out to be greater challenges than the 10^5 times larger foregrounds for intensity mapping.

7. Statistical challenges II: Calibration

The idea of using intensity mapping to reconstruct the large scale structure of the universe bring radio astronomy back to what has been one of its greatest successes—mapping out cosmological diffuse emission. Indeed, tremendous progress has been made in mapping out the cosmic microwave background (CMB) and the hope is that many

of the techniques developed there may inform us on how best to proceed. We will now briefly address some of the problems that need to be tackled if we are to move forward with this technique.

For a start, and from figure 3, it is clear that different redshift ranges will require different observation "modes": at high redshift it is preferable to use interferometers while at low redshifts it should be more efficient to work with single dishes (or "auto-correlation" mode in the parlance of radio astronomers). This is not a watertight rule. For example, with the clever use of phase arrays or cylindrical arrays, it should be possible to construct interferometers with short baselines and large fields of view hence accessing larger wavelengths at lower redshifts. But, for now, this separation of scales/redshift is useful in guiding us through the issues.

At low redshifts one needs to perform a classic CMB-like observation which is to raster scan the sky building up a rich set of cross-linked scans that cover as much area as possible with as much depth as is necessary. The key problems are then dealing with the long term drifts in the noise (the $1/f$ noise which is ubiquitous in such experiments) and accurately calibrating the overall signal. Usually, the first problem can be dealt with sufficiently fast scan speed (such that the bulk of the signal is concentrated in frequency in the regime where the $1/f$ has died off and the noise is effectively uncorrelated) but this can be difficult to achieve with large dishes such as the ones that are envisaged in current and future experiments. For some setups, the fortuitous configuration of elevation and location mean that drift scanning may lead to a fast enough scan speed.

With regards to calibrating single dish experiments, this is a source of major concern. Major systematic effects to be tackled are spillover and sidelobe pickup as well as gain drifts. Again, these are issues that have been tackled successfully in the analysis of CMB data although novel approaches can be envisaged. So, for example, the BINGO experiment (Battye *et al.* 2013) propose to use a partially illuminated aperture and a fixed single dish, minimising the problems that arise from moving parts. Another intriguing possibility is, for a cluster of single dishes working in autocorrelation mode, to use the cross correlation data for calibrating off known sources. This means that in principle, calibrating the gains should be straightforward using the interferometer data since the high resolution will allow access to a good sky model.

In the case of interferometric measurements, the challenge is to capture as much of the long wavelength modes as possible. The largest wavelength is set by the smallest baseline and in Fig. 3 we can see that arrays with large dishes will not adequately sample BAO scales at low redshift in interferometer mode. To mitigate this problem, one can work with dense aperture arrays – to just use smaller dishes and pack them closer together. This results in smaller baselines and a larger field of view for the interferometer, but reduces its total effective collecting area (and thus its sensitivity). Alternatively, one can use a more novel reflector design – for example long cylindrical reflectors with many closely-spaced receivers installed along the cylinder (Shaw *et al.* 2014). This provides a large number of short baselines, and a primary beam that is $\sim 180^\circ$ in one direction but much narrower along the orthogonal direction. Another possibility is to make interferometric measurements over a number of separate pointings without mosaicing, simply to survey a larger area of sky (White *et al.* 1999). Drift scanning can be seen as a continuous limit of this. The advantage of such a method is that one can greatly reduce the sample variance of the smallest-baseline modes, simply by observing them on several independent patches of the sky.

8. Summary

Neutral hydrogen intensity mapping looks set to become a leading cosmology probe during this decade. Intensity mapping at radio frequencies has a number of advantages over other large scale structure survey methodologies. Since we only care about the large-scale characteristics of the HI emission, there is no need to resolve and catalogue individual objects, which makes it much faster to survey large volumes. This also changes the characteristics of the data analysis problem: rather than looking at discrete objects, one is dealing with a continuous field, which opens up the possibility of using alternative analysis methods similar to those applied (extremely successfully) to the CMB. Thanks to the narrow channel bandwidths of modern radio receivers, one automatically measures redshifts with high precision too, bypassing one of the most difficult aspects of performing a galaxy redshift survey.

These advantages, combined with the rapid development of suitable instruments over the coming decade, look set to turn HI intensity mapping into a highly competitive cosmological probe. One of the key instruments that can be used for this purpose is the Phase I of the SKA. A large sky survey with this telescope should be able to provide stringent constraints on the nature of dark energy, modified gravity models and the curvature of the Universe. Moreover, it will open up the possibility to probe Baryon Acoustic Oscillations at high redshifts as well as ultra-large scales, beyond the horizon size, which can be used to constrain effects such as primordial non-Gaussianity or potential deviations from large-scale homogeneity and isotropy.

Several challenges will have to be overcome, however, if we want to use this signal for cosmological purposes. In particular, cleaning of the huge foreground contamination, removal of any systematic effects and calibration of the system. Foreground cleaning methods have already been tested with relatively success taking advantage of the foreground smoothness across frequency but novel methods need to be explored in order to deal with more complex foregrounds. Other contaminants, such as some instrumental noise bias that shows up in the auto-correlation signal, can in principle be dealt with the same methods. Ultimately, we should deal with the cleaning of the signal and the map making at the same time. This will require even more sophisticated statistical analysis methods and it will be crucial to take on such an enterprise in the next few years in order to take full advantage of this novel observational window for cosmology.

References

- Abdalla, F. B., Blake, C., & Rawlings, S. 2010, *MNRAS*, 401, 743
 Alonso, D., Ferreira, P. G., & Santos, M. G. 2014
 Ansari, R., Campagne, J. E., Colom, P., *et al.* 2012, *A. & A.*, 540, A129
 Bagla, J., Khandai, N., & Datta, K. K. 2010, *Mon. Not. Roy. Astron. Soc.*, 407, 567
 Battye, R. A., Browne, I. W. A., Dickinson, C., *et al.* 2013, *M.N.R.A.S.*, 434, 1239
 Battye, R. A., Davies, R. D., & Weller, J. 2004, *Mon. Not. Roy. Astron. Soc.*, 355, 1339
 Bernardi, G., de Bruyn, A. G., Brentjens, M. A., *et al.* 2009, *A&A*, 500, 965
 Bernardi, G., de Bruyn, A. G., Harker, G., *et al.* 2010, *A&A*, 522, A67
 Blake, C., Brough, S., Colless, M., *et al.* 2012, *MNRAS*, 425, 405
 Bull, P., Ferreira, P. G., Patel, P., & Santos, M. G. 2014, arXiv:1405.1452 [astro-ph.CO]
 Camera, S., Santos, M. G., Ferreira, P. G., & Ferramacho, L. 2013, *Phys. Rev. Lett.*, 111, 171302
 Chang, T.-C., Pen, U.-L., Bandura, K., & Peterson, J. B. 2010, *Nature*, 466, 463
 Chang, T.-C., Pen, U.-L., Peterson, J. B., & McDonald, P. 2008, *Phys. Rev. Lett.*, 100, 091303
 Chapman, E., Abdalla, F. B., Harker, G., *et al.* 2012, *MNRAS*, 423, 2518
 CHIME Collaboration. 2012, Overview, <http://chime.phas.ubc.ca/CHIME.overview.pdf>
 Dawson, K. S., Schlegel, D. J., Ahn, C. P., *et al.* 2013, *AJ*, 145, 10

- Di Matteo, T., Perna, R., Abel, T., & Rees, M. J. 2002, *ApJ*, 564, 576
- Gleser, L., Nusser, A., & Benson, A. J. 2008, *M.N.R.A.S.*, 391, 383
- Hinshaw, G., Larson, D., Komatsu, E., *et al.* 2013, *ApJS*, 208, 19
- Jelić, V., Zaroubi, S., Labropoulos, P., *et al.* 2010, *MNRAS*, 409, 1647
- Jelić, V. *et al.* 2008, *M.N.R.A.S.*, 389, 1319
- Kaiser, N. 1987, *Mon.Not.Roy.Astron.Soc.*, 227, 1
- Kerp, J., Winkel, B., Ben Bekhti, N., Flöer, L., & Kalberla, P. M. W. 2011, *Astronomische Nachrichten*, 332, 637
- Lidz, A., Furlanetto, S. R., Oh, S. P., *et al.* 2011, *ApJ*, 741, 70
- Liu, A. & Tegmark, M. 2011, *Phys. Rev. D*, 83, 103006
- Liu, A., Tegmark, M., Bowman, J., *et al.* 2009, *M.N.R.A.S.*, 398, 401
- Loeb, A. & Wyithe, J. S. B. 2008, *Physical Review Letters*, 100, 161301
- Mao, Y., Tegmark, M., McQuinn, M., Zaldarriaga, M., & Zahn, O. 2008, *Phys. Rev. D*, 78, 023529
- Masui, K. W. *et al.* 2013, *Ap. J. L.*, 763, L20
- McDonald, P. & Seljak, U. 2009, *JCAP*, 0910, 007
- McQuinn, M., Zahn, O., Zaldarriaga, M., *et al.* 2006, *ApJ*, 653, 815
- Moore, D. F., Aguirre, J. E., Parsons, A. R., Jacobs, D. C., & Pober, J. C. 2013, *ApJ*, 769, 154
- Morales, M. F., Bowman, J. D., & Hewitt, J. N. 2006, *ApJ*, 648, 767
- Obreschkow, D., Klöckner, H.-R., Heywood, I., Levrier, F., & Rawlings, S. 2009, *ApJ*, 703, 1890
- Oh, S. P. & Mack, K. J. 2003, *M.N.R.A.S.*, 346, 871
- Peterson, J. B., Aleksan, R., Ansari, R., *et al.* 2009, arXiv:0902.3091 [astro-ph.IM]
- Planck Collaboration, Ade, P. A. R., Aghanim, N., *et al.* 2013a, arXiv:1303.5062 [astro-ph.CO]
- Planck Collaboration, Ade, P. A. R., Aghanim, N., *et al.* 2013b, arXiv:1303.5076 [astro-ph.CO]
- Pritchard, J. R. & Loeb, A. 2008, *Phys. Rev. D*, 78, 103511
- Santos, M. G., Cooray, A., & Knox, L. 2005, *ApJ*, 625, 575
- Seo, H.-J., Dodelson, S., Marriner, J., *et al.* 2010, *Astrophys.J.*, 721, 164
- Shaw, J. R., Sigurdson, K., Pen, U.-L., Stebbins, A., & Sitwell, M. 2013, *ApJ*, 781, 57
- Shaw, J. R., Sigurdson, K., Sitwell, M., Stebbins, A., & Pen, U.-L. 2014, arXiv:1401.2095 [astro-ph.CO]
- Switzer, E. R., Masui, K. W., Bandura, K., *et al.* 2013, *MNRAS*, 434, L46
- Wang, X., Tegmark, M., Santos, M. G., & Knox, L. 2006, *ApJ*, 650, 529
- White, M., Carlstrom, J. E., Dragovan, M., & Holzappel, W. L. 1999, *ApJ*, 514, 12
- Wilman, R. J., Miller, L., Jarvis, M. J., *et al.* 2008, *M.N.R.A.S.*, 388, 1335
- Wolz, L., Abdalla, F. B., Blake, C., *et al.* 2014, *MNRAS*, 441, 3271
- Wyithe, J. S. B. & Loeb, A. 2008, *M.N.R.A.S.*, 383, 606
- Wyithe, J. S. B., Loeb, A., & Geil, P. M. 2008, *M.N.R.A.S.*, 383, 1195